Complex Liquid Crystal Emulsions for Biosensing

Alberto Concellón, Darryl Fong, and Timothy M. Swager*

Department of Chemistry, Massachusetts Institute of Technology, 77 Massachusetts Avenue, Cambridge, Massachusetts 02139, United States. Email: tswager@mit.edu

ABSTRACT: Herein we describe a highly responsible optical biosensor based on dynamic complex liquid crystal emulsions. These emulsions are simple to prepare and consist of immiscible chiral nematic liquid crystals (N*) and fluorocarbon oils. In this work, we exploit the N* selective reflection to build a new sensing paradigm. Our detection strategy is based on changes in the LC/W interfacial activity of boronic acid polymeric surfactants *via* reversible interactions with IgG antibodies at the LC interface. Such biomolecular recognition events can vary the pitch length of the N* organization due to the presence of binaphthyl units in the polymeric structure, which are known to be powerful chiral dopants. We demonstrate that these interface triggered reflection changes can be used as an effective optical read-out for the detection of the foodborne pathogen *Salmonella*.

INTRODUCTION

Liquid crystals (LCs) are dynamic self-assembled systems that display a unique combination of crystalline order and liquid fluidity.[1-2] The intrinsic anisotropy and facile manipulation of their alignment are enabling features for a plethora of applications, including chemical and biological sensing, optics, or soft robotics.[3-5] Confinement of LCs within micrometer-size emulsion droplets imposes constraints on the LC orientational ordering, resulting in several mesoscale organizations that are highly responsive to molecular-level perturbations that occur at the LC/water interface.[6-7] LC emulsions are therefore promising for sensing technologies, wherein the LC alignment acts as an amplifier for local perturbations resulting in optical appearance changes.[8-9] For instance, recent reports have demonstrated that LC emulsions undergo ordering transitions in response to the presence of proteins, lipids, bacteria or viruses.[10-14] However, in these LC emulsions-based sensors the observables require optical microscopies with crossed-polarizers, which can limit real-world utility. In order to simplify the optical read-out, we incorporate chiral nematic LCs to produce complex liquid emulsions that give color changes in response to pathogens. Chiral nematic (N*) LCs, also informally referred to as cholesteric LCs, are one-dimensional photonic materials that reflect light as a result of a periodic helical molecular organization. The selective reflection is directly related to the pitch of the helical organization, which can be easily changed with external stimuli (*i.e.* pH, temperature, chemical composition, etc.). This property has demonstrated utility for constructing inexpensive optical sensors that can operate under ambient light without need of a power source.[15-16]

Herein, we demonstrate that complex N* LC emulsions can be used to fabricate a new optical sensor scheme (**Figure 1**). The emulsions are dynamically reconfigurable and have two immiscible compartments composed of a N* liquid crystal and a fluorocarbon oil. The detection strategy depends on a dynamic variation of the N* pitch in response to the presence of micro-organisms. This pitch variation is achieved by using chiral polymer surfactants with boronic acid functionality. Boronic acids are widely used recognition elements that reversibly bind N-glycans present in the fragment crystallizable (Fc) region of IgG antibodies. Hence, the combination of the polymer and the antibody produces a new functional macromolecular surfactant complex. We anticipated that antibody interaction with target bacteria will produce optical changes as a result of the modulation of the chiral polymer at the LC/water interface. We demonstrate that these changes produce optically readable and triggered reflectance changes that can be used as an effective optical read-out for the detection of *Salmonella enterica* serovar Typhimurium.

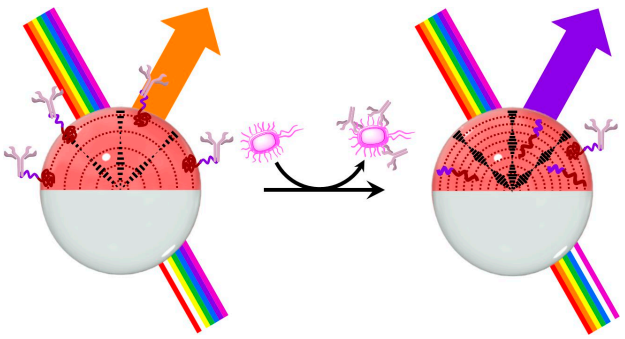

Figure 1. Schematic representation of the mechanism for *Salmonella enterica* detection using chiral nematic (N*) complex emulsions. Changes in the reflected light are produced thought changes in the interfacial activity of boronic acid polymeric surfactants, induced by a competitive binding/unbinding of IgG antibodies at the LC/W interface.

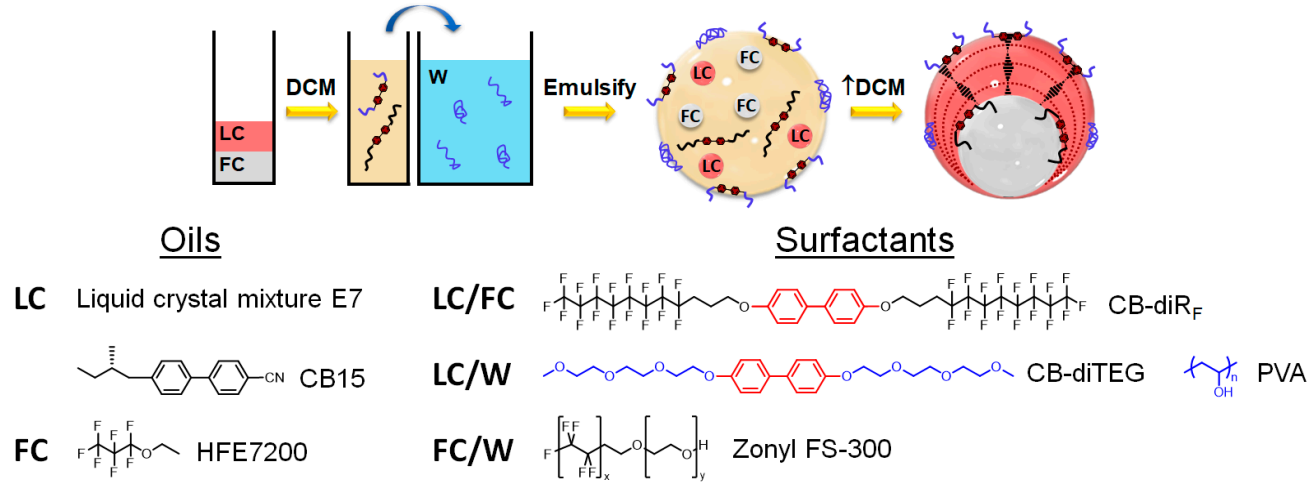

Figure 2. Schematic representation for the preparation of multicompartment emulsions comprising immiscible N* liquid crystals (LC) and fluorocarbon (FC) oils in water. In the evaporation-induced phase separation method, DCM is added to create a single phase and slowly evaporates post-emulsification to produce the phase separated complex emulsion structure.

RESULTS AND DISCUSSION

We have previously reported dynamically reconfigurable multicompartment emulsions consisting of immiscible nematic LCs and a fluorocarbon oils (FC) dispersed in water.[17] The nematic phase is the least ordered LC phase, wherein molecules only exhibit orientational order. By adding a chiral compound (dopant), helical twisting of the mesophase director is induced, leading to a N* LC phase. The main advantage of doped N* LCs is the facility with which its pitch can be modulated by changing the chiral dopant concentration. The helical twisting power (HTP) of a chiral dopant is related with its ability to twist the nematic phase, and is defined as $HTP = 1/(P \times C)$, where C is the concentration of the chiral dopant and P the helical pitch. The wavelength of the selective reflection (λ) is defined as $\lambda = n \times P \times \cos\theta$, where n is the average refractive index of the LC, and θ is the incidence angle of the light. Visible light is selectively reflected by N* phases when their pitch length is in the same regime as visible light. In this work, we chose E7 as the nematic LC matrix, and (*S*)-4-cyano-4'-(2-methylbutyl)biphenyl (CB15, HTP ≈ 7.1 μm^{-1}) as the chiral dopant. We prepared two cholesteric mixtures with different compositions of CB15 in E7, namely 1 wt % (**N*1**) and 32 wt % (**N*32**). The higher concentration gives a reflection band of the N* LC centered in the red region (P = 0.44 µm, λ = 720 nm), which is useful for investigating the emulsion's optical properties. The lower concentration produced a helical periodicity in the micrometer range (P = 14.0 µm), which can be imaged by optical microscopy.

The performance of our complex LC emulsions relies on a fine control of the LC orientation, and this can be accomplished by the incorporation of appropriately designed LC surfactants. Specifically, photonic effects in N* LC droplets are enhanced when the helical twist axis has a radial helical orientation wherein the LC molecules are parallel to the droplet aqueous interface.[18-20] The complex emulsion droplets have an internal interface and we used **CB-diR$_F$** surfactant, which stabilizes the LC/FC interface and provides a parallel (planar) alignment of the LC molecules. Planar alignment of the mesogens at the LC/W interface was achieved by using **CB-diTEG**, and poly(vinyl alcohol) (PVA). LC complex droplets were prepared by using an evaporation-induced phase separation method (**Figure 2**). Specifically, droplets were produced by emulsification of a 1:1:3 volume ratio of N*/HFE7200/dichloromethane into a 0.1 wt % solution of PVA. After complete evaporation of dichloromethane (DCM), fluorocarbon-in-LC-in-water (FC/LC/W) double emulsions were obtained. The morphology of these complex LC emulsions can be dynamically triggered in response to changes in aqueous surfactant mass balance.[17, 21] Thus, addition of an aqueous solution of Zonyl (a nonionic fluorosurfactant) transforms the droplet morphology to a Janus configuration or to a LC-in-fluorocarbon-in-water (LC/FC/W) double emulsion (**Figure 3**).

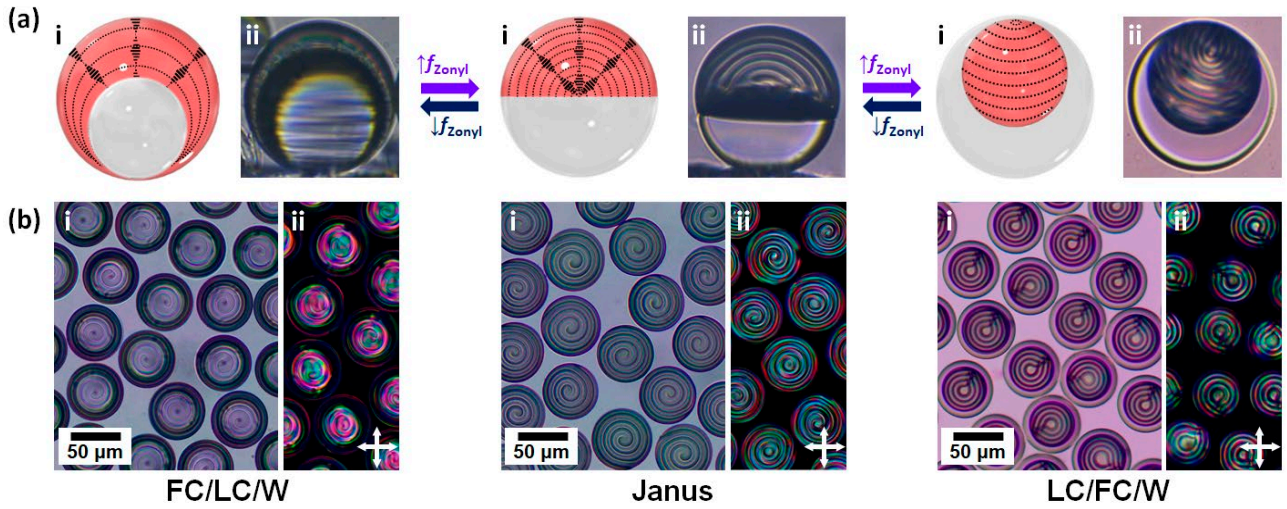

Figure 3. (a) Schematic representations (i) and side-view microscopy images (ii), **(b)** polarized-light optical microscopy images without (i) and with (ii) crossed polarizers of **N*1** complex emulsions that reconfigure in response to surfactant variations. The FC/LC/W double emulsions shown left are produced when the continuous phase has a 0.1 wt % PVA aqueous solution. The Janus droplets in the center are created in water solutions containing 0.1 wt % PVA and 0.01 wt % Zonyl, (1:9 v/v). The LC/FC/W double emulsions shown right are produced in water solutions containing 0.1 wt % PVA and 0.01 wt % Zonyl (1:1 v/v).

To gain insight about the internal structure of these chiral nematic double emulsions, we initially investigated **N*1** emulsions, since they have a helical pitch in the micrometer range that can be readily visualized by optical microscopy. Periodic dark and bright concentric rings were observed in **N*1** Janus droplets. This suggests a radial disposition of the N* helixes that originates from the equator of the droplet. This radial helical structure produces a pattern of equidistant concentric rings, whose inter-ring periodicity corresponds to $P/2$ (**Figure 3**).[22] In the case of FC/LC/W and LC/FC/W double emulsions, they also exhibited helical structures with concentric rings due to a radial disposition of the N* layers. In addition, a radial defect line was observed in LC/FC/W droplets, suggesting that all N* layers follows a group of circles, which pass through the same point (Frank-Pryce model).[23]

In contrast, the short pitch of **N*32** Janus emulsions prevents the observation of the helical organization by optical microscopy. Nonetheless, reflection-mode bright field images showed different colored patterns confirming a periodic internal structure (**Figure 4**). Specifically, **N*32** Janus droplets showed a bright central spot together with radial lines connecting these central spots. The central reflection originates from the normal reflection of the N* arrangement, whereas the less-intense radial reflections are attributed to photonic inter-droplet cross-communication.[20] These photonic patterns evidence the formation of an uniform radial helical structure within **N*32** Janus droplets. The cross-communication mechanism is shown in **Figure 4c**. When the incident light hits at an angle of 45° (blue line in **Figure 4c**), it is reflected at 45° to the adjacent droplet, and then reflected again by this droplet at an angle of 45° (depicted by the orange arrows in **Figure 4c**). To corroborate this cross-communication mechanism, we closed the illuminated area in our reflection microscope; non-illuminated droplets did not show the central reflection spot and only showed the radial reflections coming from the neighboring illuminated droplet (**Figure 4d-i**). Moreover, we isolate one and three droplets to study their reflection patterns. The isolated single droplet does not show any lateral communication, and only showed the central reflection (**Figure 4d-ii**). However, the cross-communication interactions between adjacent droplets can be readily visualized in the group of three droplets. We also noticed that the intensity of the cross-communication process depends on the distance between droplets, disappearing with large inter-droplet distances (**Figure 4d-iii**). FC/LC/W and LC/FC/W double emulsion droplets also exhibited radial helical structures. The uniform radial disposition of the N* helixes in LC/F/W double emulsions is confirmed by the presence of a central defect in the LC compartment. In addition, FC/LC/W double emulsions exhibited a colored pattern by reflectance microscopy, which is generated by photonic cross-communication between adjacent droplets, similarly to previously reported water-in-oil-in-water N* shells (**Figure 4b**).[24-25] Nonetheless, LC/FC/W did not exhibit any colored pattern due to total internal reflection across the LC/FC interface that confines all light within the fully encapsulated LC compartment (**Figure 4b**).[26]

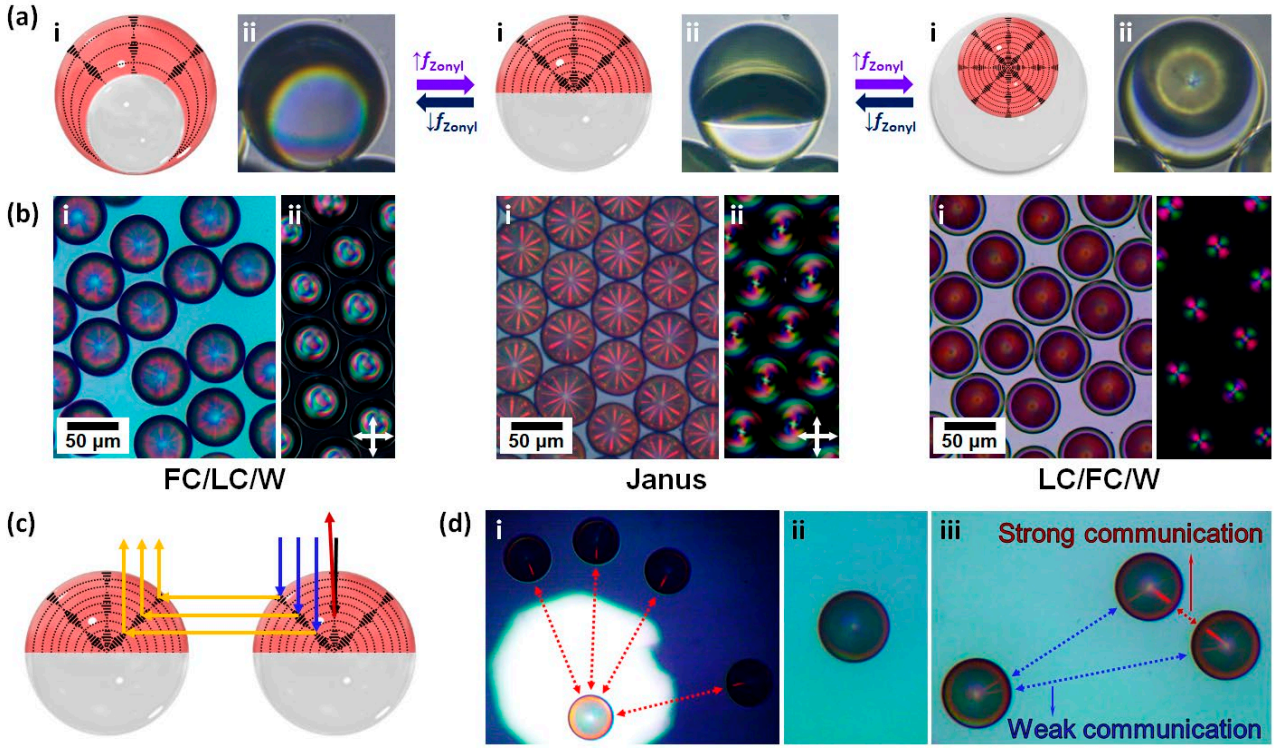

Figure 4. **(a)** Schematic representations (i) and side-view microscopy images (ii), **(b)** reflection-mode (i) and transmission-mode with crossed polarizers (ii) optical microscopy images of **N*32** complex emulsions that reconfigure in response to surfactant variations. The FC/LC/W double emulsions shown left are produced when the continuous phase has a 0.1 wt % PVA aqueous solution. The Janus droplets, in the center, are in water with 0.1 wt % PVA and 0.01 wt % Zonyl (1:9 v/v). LC/FC/W double emulsions shown in right are created in a water solution of 0.1 wt % PVA and 0.01 wt % Zonyl (1:1 v/v). Panel **(c)** provides a schematic representation of the cross-communication mechanism. In **(d)**-i the reflection-mode optical microscopy images of Janus **N*32** droplets are shown wherein focusing on a single droplet shows that light is transferred to neighboring droplets. Isolated droplets in **(d)**-ii do not display the radial lines that come from cross optical communication. In **(d)**-iii the higher intensity communication lines are observed from droplets which are closer together.

Having optimized the preparation of N* complex emulsions, we targeted their use as biosensors, wherein a change of the pitch may produce a change in the reflection wavelength. This pitch variation can be achieved by adsorbing the analyte at the LC interface or dissolving it in the LC medium, producing a physical swelling of the N* helix and a red-shift of the reflected light.[27-28] The selectivity of such sensors is therefore determined by the analyte solubility in the N* LC. However, most biomolecules or micro-organisms are not soluble in N* LCs and hence different mechanisms are needed in emulsions-based biosensors. To this end, we targeted the incorporation of IgG antibodies in our complex N* emulsions for the selective detection of *Salmonella* bacteria, a foodborne pathogen that causes gastrointestinal infection.

Side-chain LC polymer surfactants have been widely used to trigger LC ordering transitions in response to external stimuli. In these systems, changes in the polymeric assembly at the LC/W interface propagates throughout the LC, resulting in a change in the LC organization.[29-30] In our case, to generate changes in the pitch of the N* structure in response to the presence of micro-organisms we designed amphiphilic block copolymers containing LC and water soluble blocks (**Figure 5**). The LC soluble block is composed of binaphthyl motifs, known to provide a high HTP value,[31] randomly copolymerized with a cyanobiphenyl methacrylate to favor its solubility in the nematic LC matrix (binaphthyl/cyanobiphenyl weight proportion ≈ 80:20). The water soluble block has boronic acid functionalities. These multifunctional block copolymers function as cosurfactants in the emulsification process to prepare our N* droplets. The boronic acid groups are positioned at the LC/W interface for reversible binding with anti-*Salmonella* Typhimirium IgG antibodies. We have previously observed that bioconjugation with IgG antibodies results in an increase of the interfacial activity of polymeric surfactants, as the large IgG molecules (≈ 150 kDa) provide additional hydrophilic character.[32] We hypothesized that our bioconjugated surfactants would be mainly located at the LC/W interface due to their higher interfacial activity, and thus their ability to affect the helical structure of the N* LC would be much lower. In contrast, a powerful chiral dopant activity was expected for non-bioconjugated block copolymer surfactants as a result of their lower tendency to assemble at LC/W interface. Because of the high HTP of binaphthyl side-chains (an HTP value of 122 μm^{-1} was calculated for **P1**, see Supporting Information), minuscule changes in the interfacial activity of boronic acid surfactants is enough to alter the pitch of the chiral nematic organization, which can be detected by monitoring the normal reflection.

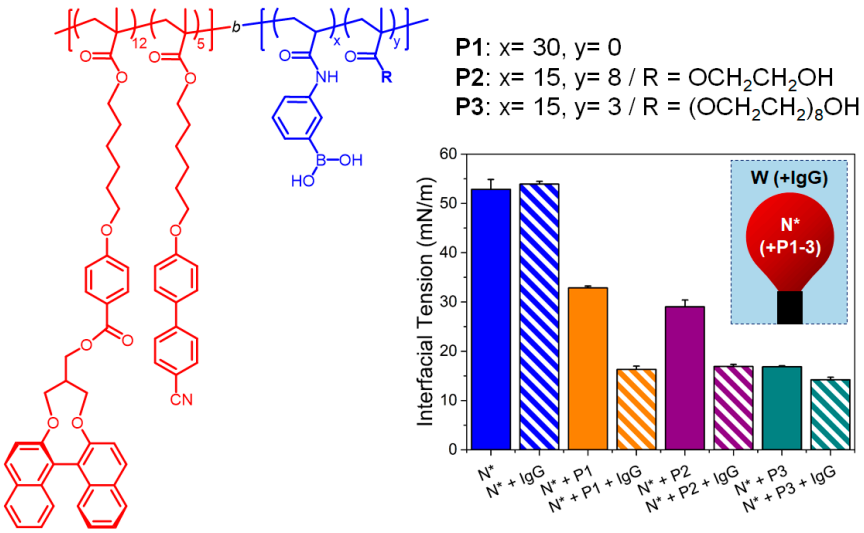

Figure 5. Chemical structures of boronic acid surfactants and pendant-drop analysis of the bioconjugation reaction. Note that the polymer-antibody complexes lower the water/N* LC interfacial tensions.

To ensure efficient dynamic assembly at the LC/W interface, we synthesized three different polymers having the same LC block, molecular weights ($M_n \approx 12$ kDa), hydrophilic/hydrophobic balance ($w_{hydrophilic} \approx 20$ wt. %), but different hydrophilic block composition (**Figure 5**). Given that we were unsure of how this structural variation in the hydrophilic block would affect polymer assembly at the LC/W interface, the surfactant ability was quantified by pendant-drop measurements. All non-bioconjugated polymers are surface active, reducing LC/W interfacial tension ($\gamma_{LC/W}$) from 52.9 mN/m to 32.9 (**P1**), 29.0 (**P2**), and 16.7 mN/m (**P3**), when 5 mg/mL of the polymer is dispersed in the N* LC. Pendant-drop studies also confirmed the impact of bioconjugation on $\gamma_{LC/W}$, since addition of anti-*Salmonella* IgG antibodies to the continuous water phase further reduces $\gamma_{LC/W}$ to 16.3 (**P1**), 16.9 (**P2**) and 14.2 mN/m (**P3**). Therefore, pendant-drop measurements revealed that polymers position boronic acid groups at the LC/W interface, which enables bioconjugation *via* boronate ester formation with the N-glycans in the Fc region of IgG antibodies, and the production of IgG-decorated N* LC droplets.

Our sensing scheme relies on changes in the interfacial activity of boronic acid surfactants associated with a competitive binding/unbinding of IgG antibodies at the LC/W interface (**Figure 6a**). Therefore, we prepared complex N* LC emulsions containing polymeric surfactant **P1**, since **P1** showed the biggest differences in $\gamma_{LC/W}$ upon bioconjugation with IgG antibodies. Janus droplets naturally gravity align on a horizontal surface as a result of the higher density of fluorocarbon phase. In this natural configuration the normal reflection can be measured by positioning a fiber-optical spectrophotometer connected to a white light over a monolayer array composed of monodisperse N* Janus emulsions (**Figure 6b**). Reflectance spectra of **N*32** droplets showed a main peak located at a wavelength of around 720 nm, which originates from the normal reflection of the cholesteric LC (**Figure 6c**). A less-intense secondary peak is also observed at around 515 nm, which is coincident with $\lambda \times \cos 45°$, due to the photonic cross-communication between droplets. Incorporation of **P1** to the LC mixture (5 mg/mL) resulted in cholesteric emulsions with a main reflection band at around 590 nm, demonstrating ability of **P1** to alter the pitch of the N* organization. Moreover, attachment of hydrophilic IgG antibodies led to a red-shifting of the main reflection band to 670 nm as a result of a major localization of **P1** at LC/W interface.

The pitch variation as a function of the concentration of heat-killed *Salmonella enterica* serovar Typhimurium (HKST) cells was quantified using the normal reflection of N* droplets. A rapid shift (*ca.* 3 h.) of the reflection band to lower wavelengths was observed after the addition of HKST cells to IgG-decorated Janus emulsions (**Figure 6c**). **Figure 6d** shows the correlation of relative reflection band and the concentration of HKST cells. The detection limit was calculated to be 10^3–10^4 cells/mL. In the control experiments under the same conditions with a block copolymer cosurfactant that does not have binaphthyl motifs in the LC block (**P1-achiral**), the reflection band did not show any change upon addition of HKST, confirming the key role of binaphthyl units in inducing changes in the helical pitch (**Figure 6d**). A second control experiment was carried out with a block copolymer that has N-hydroxysuccinimide groups instead of boronic acids (**P1-NHS**). No variation of the reflection band was observed, thereby demonstrating the importance of the reversible interfacial reactions in our sensing scheme, as **P1-NHS** forms covalent amide bonds with IgG antibodies that avoid pathogen-induced extraction of IgG from interfaces (**Figure 6d**). Therefore, this N* emulsion sensor scheme illustrates an alternative and robust strategy for detecting *Salmonella*, which can be used in a complex protein matrix.[26] Moreover, it is not limited to a particular pathogenic organism and can be adapted to a wide range of analytes without the need of specialized equipment.

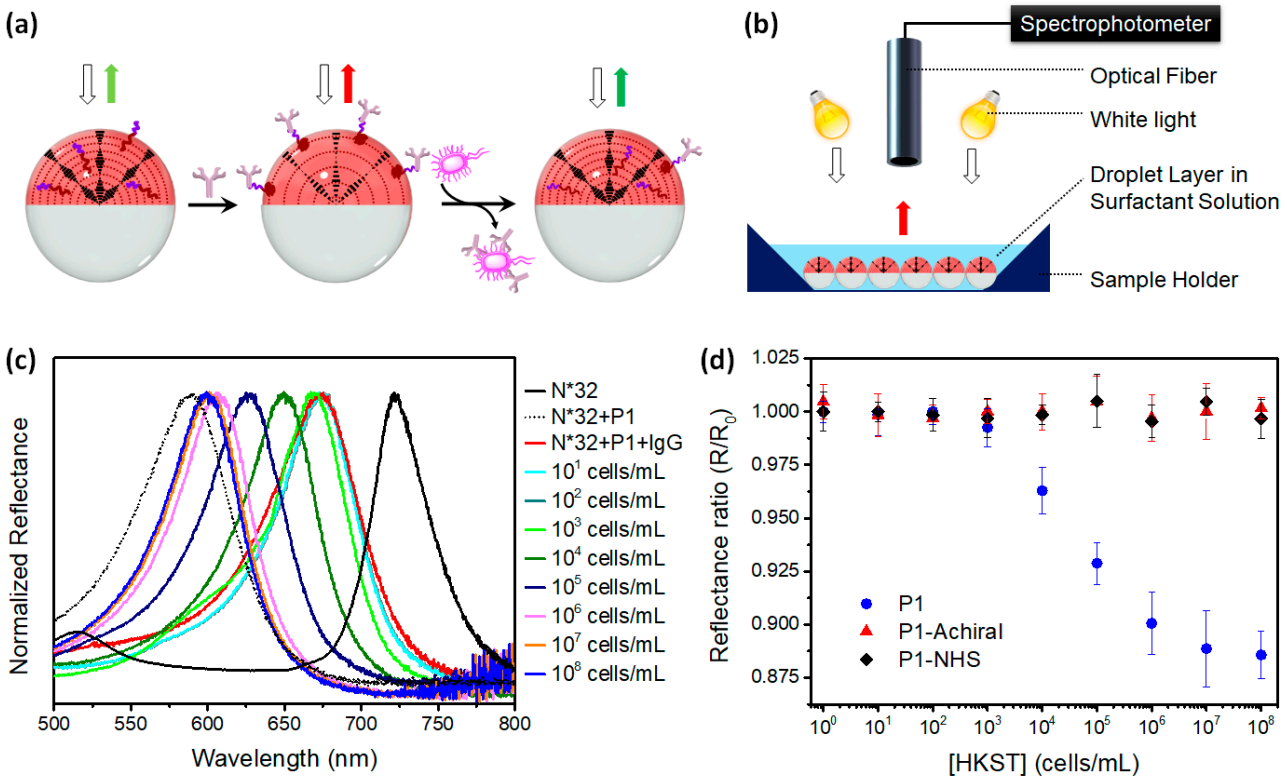

Figure 6. **(a)** Scheme of the detection mechanism for *Salmonella* using boronic acid-decorated complex N* colloids. Changes in interfacial activity of boronic acid surfactants are produced by the attachment of IgG antibodies at the LC/W interface and upon their removal by *Salmonella* cells, resulting in a variation of the pitch length. **(b)** Experimental setup for measuring the reflectance spectra of the emulsions. **(c)** Reflectance spectra of **N*32** emulsion droplets after addition of HKST at different concentrations. **(d)** Correlation of relative reflection *versus* the concentration of HKST cells.

CONCLUSIONS

We have developed complex liquid emulsions consisting of immiscible chiral nematic (N*) liquid crystals (LC) and fluorocarbon oils (FC). The morphology of these LC emulsions can be dynamically changed by varying the aqueous surfactant mass balance. Moreover, the incorporation of appropriately designed LC surfactants, which control the LC orientation at interfaces, enables the preparation of N* complex colloids with radial helical structures. The pitch length of the N* organization can be easily controlled by the amount of chiral dopant, thereby obtaining emulsions with wavelengths of reflected light. Moreover, the helical internal organization provided complex reflection patterns caused by the unique combination of selective reflection of N* LC emulsions and lateral interactions between neighboring droplets. In this work, we exploited these rich photonic properties for constructing a new sensing paradigm. Specifically, we designed boronic acid polymeric surfactants that change their LC/W interfacial activity as a result of their selective binding with IgG antibodies. Such biomolecular recognition events can vary the pitch length of the N* organization as a result of the presence of binaphthyl units in the polymeric structure, which are known to be powerful chiral dopants. These dynamic interface triggered reflection changes were used to fabricate a sensitive and quantitative detection approach for the foodborne pathogen *Salmonella*. The simple fabrication of chiral nematic emulsions and the quantitative optical read-out illustrates an alternative method for biological and chemical sensing.

ASSOCIATED CONTENT

Supporting Information. Materials and Characterization Techniques, Experimental Procedures, Synthesis and Characterization. This material is available free of charge via the Internet at http://pubs.acs.org

AUTHOR INFORMATION

Corresponding Author

* tswager@mit.edu (T. M. S)

ACKNOWLEDGMENT

This work was supported by the Vannevar Bush Faculty Fellowship (Grant No. N000141812878). D.F. is grateful for an NSERC Postdoctoral Fellowship from the Government of Canada.

REFERENCES

1. Kim, Y.-K.; Noh, J.; Nayani, K.; Abbott, N. L., Soft matter from liquid crystals. *Soft Matter* **2019**, *15* (35), 6913-6929.

2. van der Asdonk, P.; Kouwer, P. H. J., Liquid crystal templating as an approach to spatially and temporally organise soft matter. *Chem. Soc. Rev.* **2017,** *46* (19), 5935-5949.

3. Pilz da Cunha, M.; Debije, M. G.; Schenning, A. P. H. J., Bioinspired light-driven soft robots based on liquid crystal polymers. *Chem. Soc. Rev.* **2020,** *49* (18), 6568-6578.

4. Nayani, K.; Yang, Y.; Yu, H.; Jani, P.; Mavrikakis, M.; Abbott, N., Areas of opportunity related to design of chemical and biological sensors based on liquid crystals. *Liq. Cryst. Today* **2020,** *29* (2), 24-35.

5. Kato, T.; Uchida, J.; Ichikawa, T.; Sakamoto, T., Functional Liquid Crystals towards the Next Generation of Materials. *Angew. Chem. Int. Ed.* **2018,** *57* (16), 4355-4371.

6. Miller, D. S.; Wang, X.; Abbott, N. L., Design of Functional Materials Based on Liquid Crystalline Droplets. *Chem. Mater.* **2014,** *26* (1), 496-506.

7. Chen, H.-Q.; Wang, X.-Y.; Bisoyi, H. K.; Chen, L.-J.; Li, Q., Liquid Crystals in Curved Confined Geometries: Microfluidics Bring New Capabilities for Photonic Applications and Beyond. *Langmuir* **2021,** *37* (13), 3789-3807.

8. Wang, D.; Park, S.-Y.; Kang, I.-K., Liquid crystals: emerging materials for use in real-time detection applications. *J. Mater. Chem. C* **2015,** *3* (35), 9038-9047.

9. Lowe, A. M.; Abbott, N. L., Liquid Crystalline Materials for Biological Applications. *Chem. Mater.* **2012,** *24* (5), 746-758.

10. Munir, S.; Kang, I.-K.; Park, S.-Y., Polyelectrolytes functionalized nematic liquid crystal-based biosensors: An overview. *Trends Anal. Chem.* **2016,** *83*, 80-94.

11. Lin, I.-H.; Miller, D. S.; Bertics, P. J.; Murphy, C. J.; de Pablo, J. J.; Abbott, N. L., Endotoxin-Induced Structural Transformations in Liquid Crystalline Droplets. *Science* **2011,** *332* (6035), 1297-1300.

12. Sivakumar, S.; Wark, K. L.; Gupta, J. K.; Abbott, N. L.; Caruso, F., Liquid Crystal Emulsions as the Basis of Biological Sensors for the Optical Detection of Bacteria and Viruses. *Adv. Funct. Mater.* **2009,** *19* (14), 2260-2265.

13. Brake, J. M.; Daschner, M. K.; Luk, Y.-Y.; Abbott, N. L., Biomolecular Interactions at Phospholipid-Decorated Surfaces of Liquid Crystals. *Science* **2003,** *302* (5653), 2094-2097.

14. Aliño, V. J.; Pang, J.; Yang, K.-L., Liquid Crystal Droplets as a Hosting and Sensing Platform for Developing Immunoassays. *Langmuir* **2011,** *27* (19), 11784-11789.

15. Schenning, A.; Crawford, G. P.; Broer, D. J., *Liquid crystal sensors*. CRC Press: Boca Raton, FL, 2018; p xiv.

16. Mulder, D. J.; Schenning, A. P. H. J.; Bastiaansen, C. W. M., Chiral-nematic liquid crystals as one dimensional photonic materials in optical sensors. *J. Mater. Chem. C* **2014,** *2* (33), 6695-6705.

17. Concellón, A.; Zentner, C. A.; Swager, T. M., Dynamic Complex Liquid Crystal Emulsions. *J. Am. Chem. Soc.* **2019,** *141* (45), 18246-18255.

18. Schwartz, M.; Lenzini, G.; Geng, Y.; Rønne, P. B.; Ryan, P. Y. A.; Lagerwall, J. P. F., Cholesteric Liquid Crystal Shells as Enabling Material for Information-Rich Design and Architecture. *Adv. Mater.* **2018,** *30* (30), 1707382.

19. Park, S.; Lee, S. S.; Kim, S.-H., Photonic Multishells Composed of Cholesteric Liquid Crystals Designed by Controlled Phase Separation in Emulsion Drops. *Adv. Mater.* **2020,** *32* (30), 2002166.

20. Fan, J.; Li, Y.; Bisoyi, H. K.; Zola, R. S.; Yang, D.-k.; Bunning, T. J.; Weitz, D. A.; Li, Q., Light-Directing Omnidirectional Circularly Polarized Reflection from Liquid-Crystal Droplets. *Angew. Chem. Int. Ed.* **2015,** *54* (7), 2160-2164.

21. Zarzar, L. D.; Sresht, V.; Sletten, E. M.; Kalow, J. A.; Blankschtein, D.; Swager, T. M., Dynamically reconfigurable complex emulsions via tunable interfacial tensions. *Nature* **2015,** *518* (7540), 520-524.

22. Cipparrone, G.; Mazzulla, A.; Pane, A.; Hernandez, R. J.; Bartolino, R., Chiral Self-Assembled Solid Microspheres: A Novel Multifunctional Microphotonic Device. *Adv. Mater.* **2011,** *23* (48), 5773-5778.

23. Bouligand, Y.; Livolant, F., The organization of cholesteric spherulites. *J. Phys. France* **1984,** *45* (12), 1899-1923.

24. Geng, Y.; Noh, J.; Drevensek-Olenik, I.; Rupp, R.; Lenzini, G.; Lagerwall, J. P. F., High-fidelity spherical cholesteric liquid crystal Bragg reflectors generating unclonable patterns for secure authentication. *Sci. Rep.* **2016,** *6* (1), 26840.

25. Geng, Y.; Jang, J.-H.; Noh, K.-G.; Noh, J.; Lagerwall, J. P. F.; Park, S.-Y., Through the Spherical Looking-Glass: Asymmetry Enables Multicolored Internal Reflection in Cholesteric Liquid Crystal Shells. *Adv. Opt. Mater.* **2018,** *6* (1), 1700923.

26. Zeininger, L.; Nagelberg, S.; Harvey, K. S.; Savagatrup, S.; Herbert, M. B.; Yoshinaga, K.; Capobianco, J. A.; Kolle, M.; Swager, T. M., Rapid Detection of Salmonella enterica via Directional Emission from Carbohydrate-Functionalized Dynamic Double Emulsions. *ACS Cent. Sci.* **2019,** *5* (5), 789-795.

27. Lee, H.-G.; Munir, S.; Park, S.-Y., Cholesteric Liquid Crystal Droplets for Biosensors. *ACS Appl. Mater. Interfaces* **2016,** *8* (39), 26407-26417.

28. Pschyklenk, L.; Wagner, T.; Lorenz, A.; Kaul, P., Optical Gas Sensing with Encapsulated Chiral-Nematic Liquid Crystals. *ACS Appl. Polym. Mater.* **2020,** *2* (5), 1925-1932.

29. Adamiak, L.; Pendery, J.; Sun, J.; Iwabata, K.; Gianneschi, N. C.; Abbott, N. L., Design Principles for Triggerable Polymeric Amphiphiles with Mesogenic Side Chains for Multiscale Responses with Liquid Crystals. *Macromolecules* **2018**, *51* (5), 1978-1985.

30. Ma, C. D.; Adamiak, L.; Miller, D. S.; Wang, X.; Gianneschi, N. C.; Abbott, N. L., Liquid Crystal Interfaces Programmed with Enzyme-Responsive Polymers and Surfactants. *Small* **2015**, *11* (43), 5747-5751.

31. Bisoyi, H. K.; Li, Q., Light-Directing Chiral Liquid Crystal Nanostructures: From 1D to 3D. *Acc. Chem. Res.* **2014,** *47* (10), 3184-3195.

32. Zhang, Q.; Scigliano, A.; Biver, T.; Pucci, A.; Swager, T. M., Interfacial bioconjugation on emulsion droplet for biosensors. *Bioorg. Med. Chem.* **2018,** *26* (19), 5307-5313.

Insert Table of Contents artwork here